A Systematic Wideband Beamforming Approach with Low Complexity and Beamwidth Invariant Property

Qianyi Ouyang, Zhishu Qu, *Member, IEEE*, and Yue Gao, *Fellow, IEEE*

***Abstract*— In frequency domain wideband beamforming, signals are often decomposed into subbands before beamforming. For subband decomposition, existing methods can reduce the number of subbands and speed up calculation. However, their beamwidth varies with frequency and leads to signal distortion. In this paper, we propose a systematic wideband beamforming approach, which achieves beamdwidth invariant property and low computational complexity. Specifically, our contributions include: we derive the mathematics of a practical signal model and the signal transferring process in an RF (Radio Frequency) chain; we apply a novel subband decomposition method to reduce the number of subband and achieve low computational complexity; an optimization problem is designed and constraints are set to ensure a constant beamwidth among different frequencies and suppress the sidelobes. The proposed approach is simulated and verified. Simulation results show that the beamwidth stays constant and sidelobes meet our design. Also, it demonstrates a performance improvement in both the calculation time and memory usage.**

***Index Terms*—FFT (Fast Fourier Transform), Frequency Domain Beamforming, Wideband Beamforming, Signal Distortion, Subband Decomposition.**

I. Introduction

Wideband beamforming has drawn much attention due to its wide applications and future potential in various fields including radar, sonar, microphone arrays, medical imaging, and especially wireless communications[1]-[5]. The increasing requirement for services and communication throughput in scenerios including SATCOM and 5G has led to a growing signal bandwidth. Thus in wireless communications, problems related with wideband beamforming can no longer be ignored [1]-[3]. Wideband beamforming is faced with two major challenges. The first challenge is the beam squint problem [4], which means that different frequency components of a wideband signal point at different angles. The other is an increase in beamforming coefficients, representing more phase and amplitude calculations required. Methods for wideband beamforming can be separated into two categories in terms of their domain of signal processing: time domain wideband beamforming and frequency domain wideband beamforming.

One of the time domain methods is the True Time Delay (TTD) [6]-[8]. TTD aligns signals directly in the time domain and the coefficients are frequency-dependent. However, TTD requires more hardware devices. Another traditional time domain wideband beamforming structure is the Frost beamformer [9]. For a Frost beamformer, Tapped Delay Lines (TDL) are used to delay signals of each array element and thus the signal can be uniformly processed over the entire frequency band [10]. Nonetheless, to ensure narrow beams and ideal interference cancellation, a large number of time delay filters are necessary, which add design complexity to the system. More importantly, a common problem with time domain structures is the inaccuracy of time delay, which leads to a decrease in beamforming performance.

In comparison, a frequency domain method avoids the problems of filter design and time inaccuracy. Generally, signals are changed from the time domain into the frequency domain and separated into frequency subbands, then beamforming is conducted in each narrow subband [11]-[12]. Additionally, frequency domain beamforming algorithm design becomes more flexible utilizing signal processing techniques. The computational efficiency of the decomposition method depends on the number of subbands. In other words, the fewer the subbands, the fewer narrowband beamforming to be performed. Thus, the methods of subband decomposition are worth studying.

Researchers have studied both the frequency subband decomposition method and frequency domain beamforming algorithm [13]-[18]. Typically, Fast Fourier Transform (FFT) transforms the signal into the frequency domain [13]. Moreover, it naturally decomposes the signal into uniform subbands. In [14], a non-uniform decomposition method (NUDM) is proposed. Instead of simply decomposing the signal into uniform subbands, this method further reduces subbands into a nonuniform format according to a relative bandwidth theorem. The problem with this research is the variant beamwidth among subbands. This leads to signal distortion when the signal is not located precisely at the pointed angle. Its signal model, on the other hand, does not fit into a practical situation. To solve the

This work was supported by the China Postdoctoral Science Foundation under Grant 2023TQ0076. (Corresponding author: Zhishu Qu.)

Qianyi Ouyang, Zhishu Qu and Yue Gao are with the School of Computer Science, Fudan University, Shanghai 200437, China (e-mail: zhishu_qu@fudan.edu.cn).

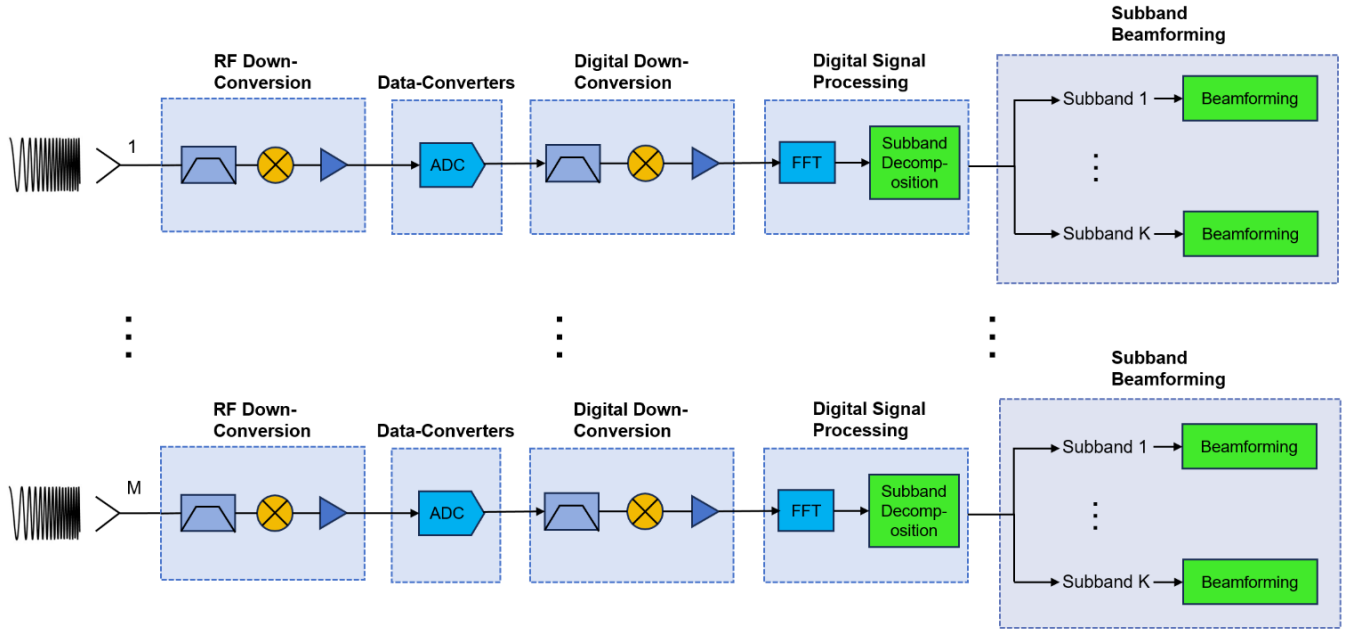

Fig. 1. An illustration of the system structure.

beamwidth variance problem, a kind of algorithm called frequency invariant beamforming (FIB) has been proposed and studied [15]-[18]. [16] achieves constant beamwidth by substituting variables in the objective function, which eliminates the frequency effect. In [17], a systematic approach based on convex optimization is proposed. However, a common problem with these works is that they do not consider the calculation complexity of their FIB algorithms. The complexity of the FIB algorithm is increased in two cases. The first case is when more subbands are required for ideal beamforming performances [16]. The second is when more constraints are added to ensure a constant beamwidth [17].

This paper presents a systematic beamwidth invariant beamforming approach with low complexity. The methametical derivation of the signal model and the RF chain is formulated. We use FFT as the uniform subband decomposition method. Then the subbands are reduced according to a relative bandwidth principle, which reduces the additional computational complexity. For each subband, a frequency-invariant beamforming algorithm is designed to keep a constant beam shape among the frequency band. Simulation results show that this approach keeps a constant beamwidth, which avoids signal distortion and suppresses sidelobes. Also, it has lower computational complexity in terms of calculation time (25.6% improvement) and memory usage (25.5% improvement).

The paper is organized as follows: In Section II, our system model is formulated. Specifically, the mathematical derivation of our signal model, the subband decomposition, and the FIB algorithm design are presented. The beamwidth-variant issue is also discussed in Section II. In Section Ⅲ, the simulation results of our algorithm are presented. The conclusion is given in Section Ⅳ

.

II. Models and Principles

Our system structure is illustrated in Fig.1. The receiving signal is a wideband signal whose bandwidth can be modified. The signal goes through an RF (Radio Frequency) chain which contains RF and digital down-converters and ADCs (Analog to Digital Converter). The above is discussed in subsection-*A*. Then the signal is transferred into the frequency domain by FFT (Fast Fourier Transform) and decompose into frequency subbands. A subband decomposition method further reduces the number of subbands. These two processes are shown in the digital signal processing block, and will be discussed in subsection-*B*. For each decomposed subband, an FIB (Frequency Invariant Beamforming) algorithm is designed, formulated in subsection-*C*.

Since the signal is transferred into the frequency domain after FFT, in the following sections we focus on the frequency domain subband decomposition method and beamforming.

A. Wideband Signal Model

As mentioned, DFT (Discrete Fourier Transform)/FFT is necessary in frequency domain wideband beamforming because it converts the time domain signal into the frequency domain. This paper considers the down-converting and sampling process, which matches a practical condition (for example, the RF chain in wireless communications). Suppose that the receiving signal is a wideband signal with a carrier frequency of f_0, which can be denoted as:

$$s(t) = rect(\frac{t}{T_p})d(t)\exp\left(j2\pi f_0 t\right) \quad (1)$$

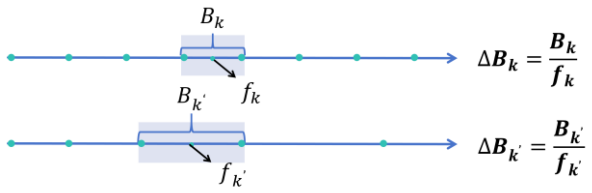

Fig. 2. An illustration of the nonuniform subband decomposition.

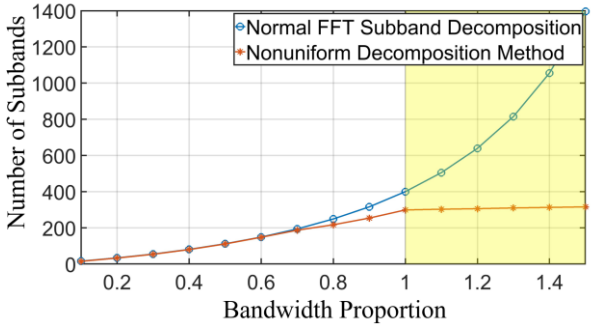

Fig. 3. The effect of different decomposition methods on the number of subbands, the x-axis (bandwidth proportion) denotes the ratio of signal bandwidth to the carrier frequency.

where *d(t)* is the complex envelope of the baseband signal, $exp(j2\pi f_0 t)$ signifies the impact of carrier frequency on the signal phase, and:

$$rect(\frac{t}{T_p}) = \begin{cases} 1, & |t| \le T_p/2 \\ 0, & others \end{cases} \tag{2}$$

This pulse signal is a common wideband pulse signal in an array system [6], whose bandwidth can be adjusted by varing T_p.

For simplicity, we consider a uniform linear array with *M* elements and element distance *d*. The receiving signal arrives at angle θ. Let $A(t) = rect(\frac{t}{T_p})d(t)$. Choosing the first array element as the reference, the signal from angle θ received by the *ith* array element can be expressed as:

$$x_i^\theta(t) = A(t+\tau_i^\theta)\exp\left[j2\pi f_0(t+\tau_i^\theta)\right] \tag{3}$$

where $\tau_i^\theta = \frac{(i-1)d\sin\theta}{c}$ signifies the time delay on array *i*. *c* is the speed of the electromagnetic wave. Note that this delay cannot be expressed in phase format due to the wideband signal property.

Then, the signal is down-converted through a mixer by multiplying an oscillating signals. This process can be simplified as elimination of time-related phase shift in the carrier term $\exp(j2\pi f_0 t)$, the signal therefore becomes:

$$x_i^\theta(t) = A(t+\tau_i^\theta)\exp(j2\pi f_0\tau_i^\theta) \tag{4}$$

The signal after sampling can be expressed by changing *t* in (4) with nT_s, where T_s is the sample period. It must be noted that the sampling rate, denoted as $1/T_s$ should be large enough to avoid signal aliasing. Thus (4) becomes:

$$x_i^\theta(n) = A(nT_s+\tau_i^\theta)\exp(j2\pi f_0\tau_i^\theta) \tag{5}$$

Rewriting x_i^θ for simplicity and generality, we have:

$$x_i^\theta(n) = \mathrm{s}(n)\mathrm{s_c}(f_0) \tag{6}$$

where $s(n) = A\left(nT_s+\tau_i^\theta\right)$ is the signal waveform, $s_c(n) = \exp\left[j2\pi f_0\tau_i^\theta\right]$ is the component introduced by the carrier.

Next, the signal is converted into the frequency domain through FFT. For simplicity, a *K*-point FFT is used to formulate a frequency domain signal model. A frequency domain x_i^θ can be simplified as:

$$X_i^\theta(f_k) = \mathrm{S}(f_k)\mathrm{s_c}(f_0), k = 1,2,...,K \tag{7}$$

where f_k is the *kth* point in the frequency domain. Note that $s_c(f_0)$ is time invariant and thus stays the same after FFT. This matters because down-sampling cannot eliminate the effect of carrier component on the final beamforming, i.e. this phase shift should be compensated by digital baseband beamforming.

Now we have a frequency domain baseband signal with uniform subbands. Next we discuss the reduction of subbands by using nonuniform decomposition.

B. Subband Decomposition

Consider our model in Section II. Suppose that (7) is already uniformly decomposed into *K* subbands by FFT. To ensure an ideal beamforming performance, the relative bandwidth should satisfy the following [14]:

$$\Delta B \le \frac{2.78c}{\sqrt{3}\pi M f_{\max}} \tag{8}$$

where the relative bandwidth $\Delta B = \Delta B_k = \frac{B_k}{f_k}$, B_k and f_k is the bandwidth and central frequency of the *kth* subband, respectively.

An illustration of the principle is shown in Fig.2. The upper line is the original uniform decomposition, where the frequency bands are equally wide and the relative bandwidth is increasing. The lower line denotes the reduced subbands, where all subbands have the same relative bandwidth ($\Delta B_{k'} = \Delta B_{k+1'}, k = 1,2,...$). Thus with the increase in $f_{k'}$, $B_{k'}$ can increase accordingly, leading to fewer subbands.

This method significantly reduces the number of subbands. Computational complexity is thus reduced because fewer narrow bands lead to fewer subband beamforming calculations. Let the relative bandwidth reach the upper limit of (8) for the

most complexity reduction, thus each subband has the same relative beamwidth. In detail, we define:

$$q = \left(\frac{2+\Delta B}{2-\Delta B} \right) \tag{9}$$

The central frequency of the *kth* subband satisfies:

$$\hat{f}_k = \frac{(q+1)\,\hat{f}_{\min}}{2} q^{k-1} = \hat{f}_1 q^{k-1} \tag{10}$$

where $\hat{f}_1$ is the lowest frequency after FFT.

The subbands are reassigned according to (10). K subbands in (7) are reduced to $\hat{K}$. We show the effectiveness of our decomposition strategy in Fig.3. The bandwidth proportion B/f_c denotes the ratio of the whole signal bandwidth to the carrier frequency (the central frequency of the whole signal with carrier). For the baseline, subbands are separated uniformly by FFT according to the upper limit in (8). For the case with nonuniform decomposition, we use (10) to separate subbands. The yellow region is highlighted, where our decomposition method shows great advantages over normal FFT.

C. Beamwidth Problem

After subband decomposition, the original wideband signal has been transferred into several narrowband signals to which normal beamforming algorithms can be applied. However, normal algorithms have different beam widths among separated narrow bands, leading to a signal distortion problem. This issue is formulated as follows:

The directional gain of an array with M is:

$$G(f,\theta) \quad = \frac{1}{M^2} \left| \sum_{m=1}^{M} \exp[\, j2\pi(m-1) \frac{df}{c} \left(\sin\theta - \sin\theta_0 \right)] \right|^2 \tag{11}$$

This expression indicates that if the signal arrives from θ instead of accurately from θ_0, the gain becomes related to the frequency component. We next demonstrate how this issue is related to the beamwidth.

Approximating the expression by assuming θ to be close to θ_0 and define the beamwidth to be the angle range where the gain loss is under 3db, which yields the following equation:

$$\frac{\sin\left[\pi M \frac{df}{c} \left(\sin\theta - \sin\theta_0 \right) \right]}{\pi M \frac{df}{c} \left(\sin\theta - \sin\theta_0 \right)} = \frac{1}{\sqrt{2}} \tag{12}$$

Qualitatively speaking, as f increases, θ gets closer to θ_0, which means a decrease in beam width. In practice when the signal is not located precisely in the beam-pointed direction, the gain varies with frequency, which leads to signal distortion.

D. FIB design

To avoid beamwidth inconsistency, a frequency invariant beamforming algorithm is designed to ensure a constant beam shape within the signal frequency band. In each subband, an optimization problem is designed to keep the same beam shape. The steering vector of a linear array with M element is defined as:

$$a(\theta, f) = [1, ..., exp(-2\pi\tau_i^{\theta} fj), ..., exp(-2\pi\tau_M^{\theta} fj)]^{\top}, i = 1, ..., M \tag{13}$$

where $\tau_i^{\theta} = \frac{(i-1)d\sin\theta}{c}$.

Note that since the signal becomes narrowband after subband decomposition, the array time delay can be expressed as phase format. Discretizing θ into P points, and substituting f with $\hat{f}_k$, (13) becomes:

$$a(\theta_p, \hat{f}_k) = [1, ..., exp(-2\pi\tau_i^{\theta_p} \hat{f}_k j), ..., exp(-2\pi\tau_M^{\theta_p} \hat{f}_k j)]^{\top}, \quad i = 1, ..., M,\ p = 1, ..., P \tag{14}$$

where $\theta_p = [\theta_1, \ldots, \theta_P]$.

Recalling (7), after nonuniform decomposition, the frequencies are redistributed, which yields:

$$X_i^{\theta}(\hat{f}_k) = \mathrm{S}\left(\hat{f}_k \right) \mathrm{s_c}\left(f_0 \right), k = 1, 2, ..., \hat{K} \tag{15}$$

Thus, the optimization target is to design a set of W for M array elements and $\hat{K}$ subbands, defined as:

$$W_{M \times \hat{K}} = [W_1, ..., W_{\hat{K}}] \tag{16}$$

where $W_{\hat{k}}$ denotes the coefficients for the $\hat{k}th$ subband, which is:

$$W_{\hat{k}} = [w_{\hat{k}1}, ..., w_{\hat{k}m}]^{\top} \tag{17}$$

To calculate the directional gain in each subband, we have:

$$G(\theta, \hat{f}_k) = W_{\hat{k}}^H a(\theta_p, \hat{f}_k) \tag{18}$$

Inspired by [19], we design an optimization algorithm. The basic principle is to set a standard narrowband main beam pattern and minimize the differences between beams in other subbands with the standard main beam. For sidelobes in each subband, a constraint keeps them under a certain level. The idea is that optimizing the beam pattern of all angles leads to a non-convex problem and is hard to solve. The optimization problem is thus defined as:

$$\min_{\mathbf{w}} \sum_{\mathrm{p}=P_{ml}}^{P_{mr}} \left[\lambda_p \left| W^H a\left(\theta_p\right) - p\left(\theta_p\right) \right|^2 \right]$$

$$\textbf{s.t.} \qquad \left| W^H a\left(\theta_i\right) \right| \le \xi_{0i}, i = 1, ..., P_{ml}, P_{mr}, ...I \tag{19}$$

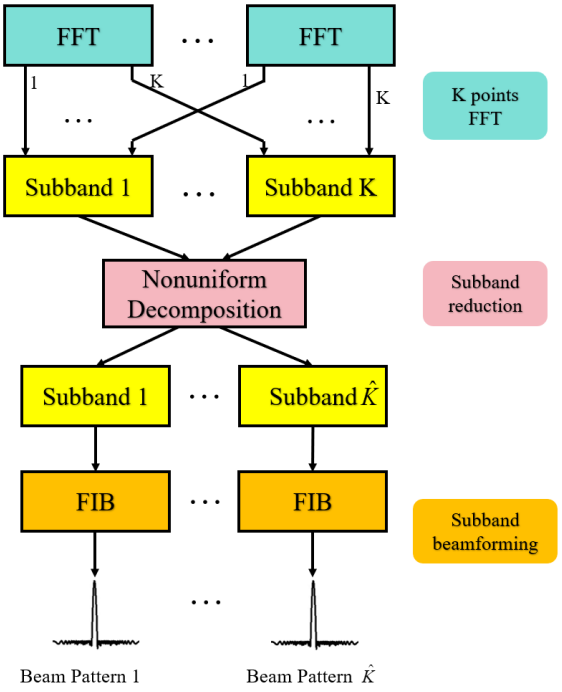

Fig. 4. A flow chart of our algorithm.

$$\| W\|_2 \le \zeta_0 \tag{20}$$

$$W^{\mathrm{H}} a_0 = g \tag{21}$$

where $p(\theta)$ is the settled standard beam pattern. We generate one according to (11). λ_p is a non-negative weight coefficient and is set to be 1 here. Among in total I sampled angle points, θ_p is the mainlobe angle, with P_{ml} and P_{mr} being the left and right bound of the mainlobe region. θ_i is the sidelobe angle. The objective function is to minimize the mean-square error between calculated mainlobe directional gain and the standard one and get W, which is the array coefficients for a subband. Constraint (19) ensures all sidelobes are lower than ξ_{0i}. (20) is a power constraint and (21) prevents frequency distortion by setting a uniform gain at the pointing angle. According to [20], this problem can be transferred into a second order cone programming. However, CVX toolbox [21] offers a direct way to get the solution of any convex problem, so here only the convex property is analyzed.

First, the original mean-square error minimization function is the summation of convex quadratic terms, which is convex. (19) contains $[I-(P_{mr}-P_{ml})-1]$ inequalities and each of them represents a convex set. (20) defines a 2-norm cone and is thus convex. In (21), $(W^{\mathrm{H}} a_0 - g)$ is an affine function of W, leading to a convex set. With the objective function and feasible sets being convex, the optimization problem is convex and can be solved easily.

The subband signal is denoted as

$$s(\hat{f}_k) = W(\hat{k})^H X^{\theta}(f_k) \tag{22}$$

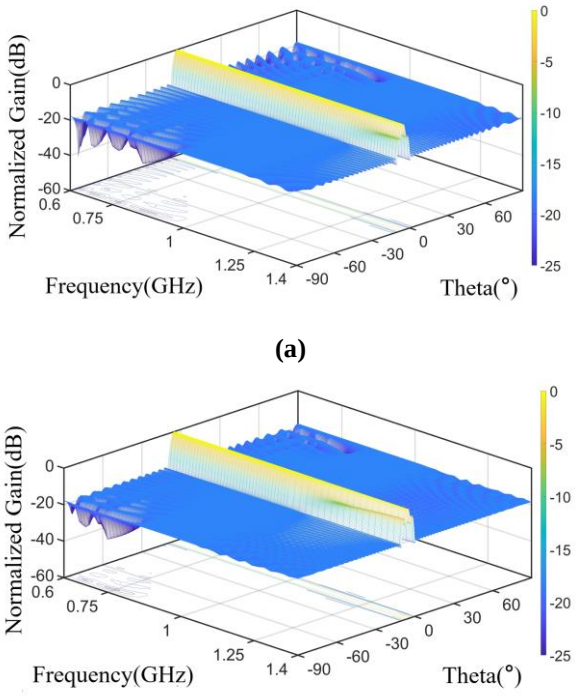

Fig. 5. 3D figure of beamforming results. (a) The result of normal Frequency Invariant Beamforming with FFT, and (b) result of our proposed algorithm.

where $X^{\theta}(f_k) = [X_1^{\theta}(f_k), ..., X_M^{\theta}(f_k)]$.

Fig.4 illustrates our algorithm flowchart, the process of subband decomposition and how beamforming is conducted are illustrated. A K-point FFT transfers the signal into the frequency domain and the signal is decomposed into K subbands. Then a nonuniform decomposition process reduces the number of subbands to $\hat{K}$. For each subband, the designed FIB forms narrow band beams with the same beamwidth.

III. Simulation Results

Simulations and several comparisons are conducted to verify the performances and advantages of our design. The results are shown from both the beam shape (directional gain) of different frequencies and the signal distortion perspectives. The computational performance of the proposed algorithm is also evaluated to demonstrate the effectiveness of our design. The simulation setups are as follows: A uniform linear array with 32 elements is used to receive signals. The distances between elements are half the wavelength of the carrier. The carrier frequency is 1GHz and the signal bandwidth is 1GHz (which promises a detectable wideband effect). The signal is arriving from -5°, with a signal–to–noise ratio of 20dB. The signal is first decomposed into $J = 94$ subbands through FFT, where J is calculated according to (8).

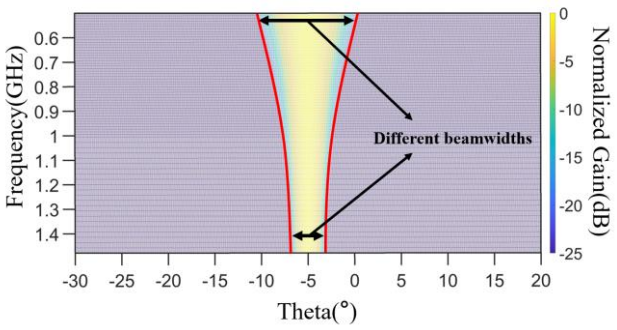

(a)

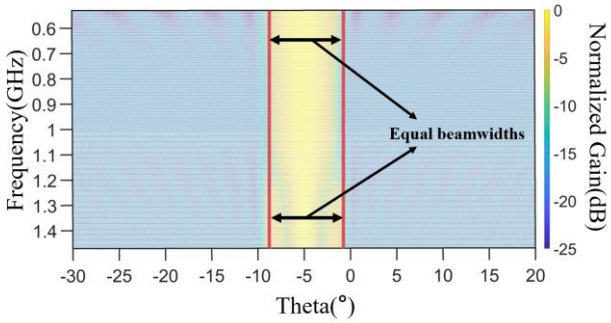

(b)

Fig. 6. 2D figures of different beamforming algorithms. (a) The Linearly Constrained Minimum Variance algorithm and (b) our proposed algorithm.

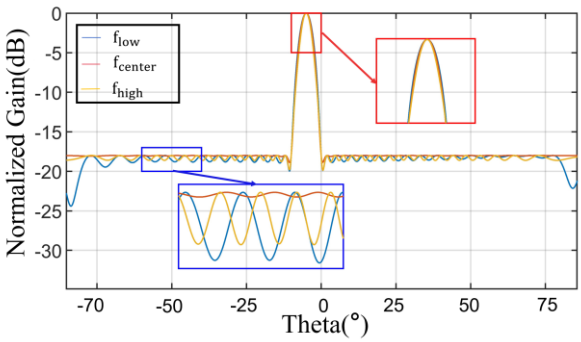

Fig. 7. Plots of beams of different frequencies.

A 94-point FFT can be feasible by conducting zero-padding, also the FFT function in Matlab and do not require the points to be the power of 2. Since we aim to evaluate the effectiveness of our algorithm, we do not force the number of subbands to be the power of 2.

After nonuniform decomposition, the number of subbands is reduced to $J' = 70$, as discussed in section 3. For the optimization problem, we normalize the directional gain and set g to be 1. The sidelobe level ξ_{0i} is -18dB and total power ζ_0 is M. The mainlobe is set to be 10°. These settings ensure the optimization problem has a solution under CVX.

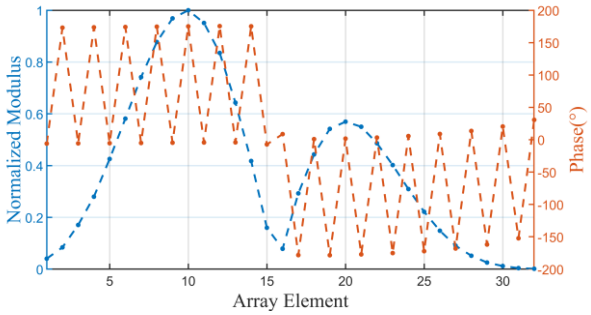

(a)

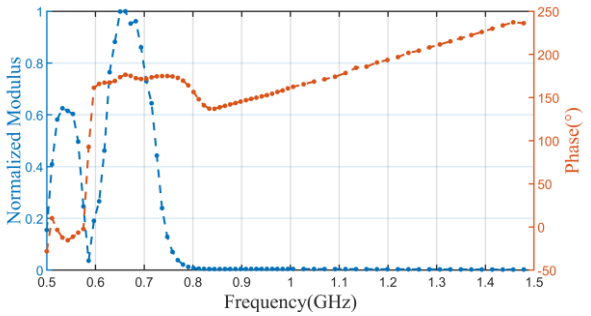

(b)

Fig. 8. Calculated normalized beamforming weights. (a) The weights of all the array elements for the 0.73GHz subband and (b) the weights for all the subbands of array element No.10.

Fig.5 shows the 3D figures of normal FIB (Frequency Invariant Beamforming) results with FFT (Fast Fourier Transform) as the subband decomposition method and the result of the proposed algorithm. (a) is normal FIB results, with 94 subbands. (b) is the result of the proposed algorithm, with 70 subbands. This demonstrates that although subbands are reduced from 94 to 70, the beam quality stays nearly the same.

Also, to show that our algorithm avoids beam width variance, our algorithm is compared with the Linearly Constrained Minimum Variance (LCMV) algorithm [14], with both 70 subbands. The results are shown in Fig.6. The main beam is marked out by red curves. The black lines with double-headed arrows show beamwidths of different frequencies. With LCMV, the beamwidths within the frequency band are different, while with our algorithm the beamwidth stays the same among different frequencies, and the sidelobes of all angles are kept under around -18dB.

Fig.7. shows beams of different frequencies. The proposed algorithm has a constant main beam width. It can be seen that the sidelobes are kept under -18dB. The main beamwidth is 10° , which meets our design. It is verified that our design has the frequency invariant property.

The results of calculated normalized beamforming weights are presented as well. The array has 32 elements, with 70 nonuniform subbands, thus the size of weights matrix is 32*70. Both the weights of one array element and one subband is shown in Fig. 8. We also show a heatmap of the modulus and phase of beamforming weights in Fig. 9 and Fig.10, respectively.

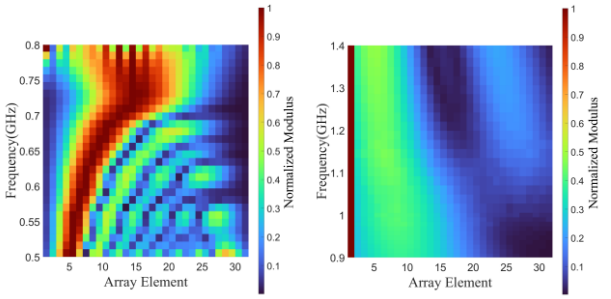

(a) **(b)**

Fig. 9. The heatmap of the normalized modulus of beamforming weights. (a) The lower frequency from 0.5 to 0.8GHz and (b) the higher frequency from 0.9 to 1.4GHz.

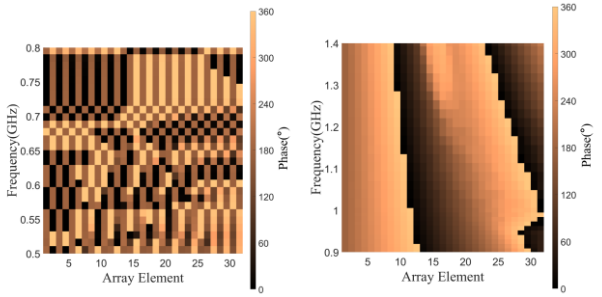

(a) **(b)**

Fig. 10. The heatmap of the phase of beamforming weights. (a) The lower frequency from 0.5 to 0.8GHz and (b) the higher frequency from 0.9 to 1.4GHz.

Recall that the purpose of conducting FIB is to avoid signal distortion. To evaluate distortion, we let a test signal arrive at $-7°$ (ideally $-5°$). Since the designed beam is pointing at $-7°$, the test signal is not exactly pointed by the main beam and will suffer a gain loss. This loss should be constant to prevent frequency distortion. Fig.11 is the frequency-gain figure when the signal arrives at $-7°$, showing the signal gains of different frequency components. The traditional LCMV algorithm whose beam widths vary with frequencies, is considered as a comparison. The normalized signal gain of different frequencies of each algorithm is shown in Fig.11. The blue line denotes a zero-distortion curve. It can be seen that both algorithms have gain losses of around 2.5dB, which results from the mismatch of the beam pointing angle with the practical arriving signal. Despite this unavoidable gain loss, the gain of our algorithm has less drop and is more stable, which mitigates the signal distortion. In contrast, the gain of the LCMV decreases as the frequency increases, as discussed in Section Ⅱ-*C*.

The above simulations are conducted when the beam is pointing at -5°. We further demonstrate that the algorithm has ideal performance in case of other beam angles. Fig.12 shows a scanning beam pattern of low, central and high frequency subbands.

At last, the computational performance of our algorithm is evaluated. We conduct our simulations using MATLAB R2023a. The computer hardware configuration is listed. CPU: 13th Gen Intel(R) Core (TM) i7-13700KF, 3400Mhz. Memory: 32 GB. Operating system: Windows.

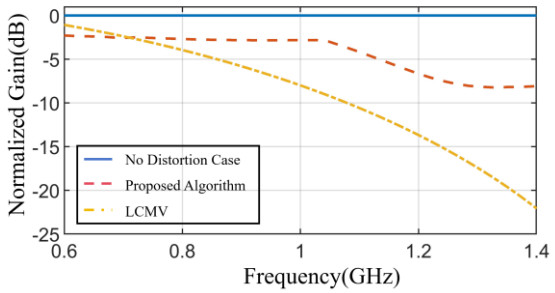

Fig. 11. The signal distortion of different algorithms.

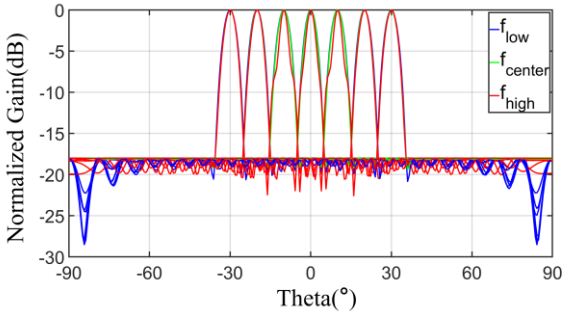

Fig. 12. The scanning beam pattern of different frequencies.

TABLE I
ALGORITHM PERFORMANCE COMPARISON

Bandwidth Proportion	Calculation Time(s)		Memory Usage(Bytes)	
	FIB+ FFT	Proposed Algorithm	FIB+ FFT	Proposed Algorithm
0.2	1.42	1.25	4608	4096
0.6	5.53	5.39	18432	17920
1.0	14.37	10.69	48128	35840
1.4	38.11	18.47	126976	60416
1.8	294.69	57.37	544768	106496

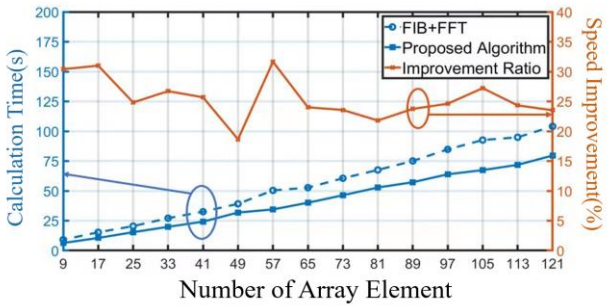

Fig. 13. The relationship between the calculation time and the number of array elements of two algorithms.

TABLE Ⅰ shows the calculation times and memory usage of two algorithms: FIB with FFT as subband decomposition and our algorithm. The signal central frequency is 1GHz and the signal bandwidth varies from 0.1GHz to 1.9GHz. Data of five frequencies is listed in the table. We do it three times and take the average as the final result. It can be seen that our algorithm takes advantages over FIB+FFT, and the advantages increase as the signal bandwidth gets larger. This results from a reduction of subbands and the trend fits Fig.3. When the bandwidth

proportion is 1, our algorithm exhibits a 25.6% performance improvement in calculation time, and saves 25.5% memory space.

Fig.13 illustrates the relationship between calculation time and the number of array elements. It shows that while the calculation time grows linearly with an increase of array elements, our algorithm has a lower increase rate and saves more than 20s when the number of array elements reaches 128.

IV. Conclusion

This work proposed a systematic wideband beamforming approach with low complexity. A common wideband signal is used to model the process of signal down-conversion and sampling. Then FFT (Fast Fourier Transform) transfers the signal from the time domain into the frequency domain. Also, the FFT decomposes the signal into uniform subbands. To reduce the number of suubands, a nonuniform decomposition method is utilized. For each subband, an FIB (Frequency Invariant Beamforming) algorithm is designed. Simulation results demonstrate the beamwidth invariant property of our design. The mainlobe of each beam is 10°, and the sidelobes are under -18dB, which all meet the designed FIB algorithm. It is also shown that the design has an improvement in computational performance. It is illustrated that the calculation time of our proposed algorithm has a growing advantage over the traditional method with the increase in the number of array elements. Specifically, there is a 25.6% performance improvement in calculation time. The memory usage has a 25.5% reduction.

References

[1] Gao F, Wang B, Xing C, et al. “Wideband beamforming for hybrid massive MIMO terahertz communications,” IEEE Journal on Selected Areas in Communications, 2021, 39(6): 1725-1740.

[2] Sikri D, Jayasuriya R M. “Multi-beam phased array with full digital beamforming for SATCOM and 5G”. Microwave Journal, 2019, 62(4): 64-79.

[3] E. H. Mujammami, I. Afifi and A. B. Sebak, "Optimum Wideband High Gain Analog Beamforming Network for 5G Applications,". IEEE Access, vol. 7, pp. 52226-52237, 2019, doi: 10.1109/ACCESS.2019.2912119.

[4] Paulson C N, Chang J T, Romero C E, et al. “Ultra-wideband radar methods and techniques of medical sensing and imaging,” in Smart Medical and Biomedical Sensor Technology III. SPIE, 2005, 6007: 96-107.

[5] Pan J. “Medical applications of ultra-wideband (uwb),” survey paper, 2007.

[6] T. Li and X. Wang, "Wideband digital beamforming by implementing digital fractional filter at baseband," 2013 International Conference on Communications, Circuits and Systems (ICS), Chengdu, China, 2013, pp. 182-185, doi: 10.1109/ICCCAS.2013.6765314.

[7] M. Longbrake, "True time-delay beam steering for radar," 2012 IEEE National Aerospace and Electronics Conference (NAECON), Dayton, OH, USA, 2012, pp. 246-249, doi: 10.1109/NAECON.2012.6531062.

[8] Horvat D C M, Bird J S, Goulding M M. “True time-delay bandpass beamforming,” IEEE Journal of Oceanic Engineering, 1992, 17(2): 185-192.

[9] Frost O L. “An algorithm for linearly constrained adaptive array processing,” Proceedings of the IEEE, 1972, 60(8): 926-935.

[10] Duan H, Ng B P, See C M S, et al. “Broadband beamforming using TDL-form IIR filters”, IEEE Transactions on Signal Processing, 2007, 55(3): 990-1002.\newline

[11] Liu W, Weiss S. “Subband Adaptive Beamforming,” in “Wideband beamforming: concepts and techniques” , John Wiley & Sons.Ltd, 2010, pp. 61-70.

[12] Harteneck M, Weiss S, Stewart R W. “Design of near perfect reconstruction oversampled filter banks for subband adaptive filters,” IEEE Transactions on Circuits and Systems II: Analog and Digital Signal Processing, 1999, 46(8): 1081-1085.

[13] Godara L C. “Application of the fast Fourier transform to broadband beamforming,” The journal of the acoustical society of America, 1995, 98(1): 230-240.

[14] Shurui Zhang, Jeyarajan Thiyagalingam, Weixing Sheng, Thia Kirubarajan, Xiaofeng Ma, “Low-complexity adaptive broadband beamforming based on the non-uniform decomposition method,” Signal Processing, Volume 151, 2018, Pages 66-75, ISSN 0165-1684,

[15] D. B. Ward, R. A. Kennedy and R. C. Williamson, "FIR filter design for frequency invariant beamformers," in IEEE Signal Processing Letters, vol. 3, no. 3, pp. 69-71, March 1996, doi: 10.1109/97.481158.

[16] W. Liu and S. Weiss, "Design of Frequency Invariant Beamformers for Broadband Arrays," in IEEE Transactions on Signal Processing, vol. 56, no. 2, pp. 855-860, Feb. 2008, doi: 10.1109/TSP.2007.907872.

[17] Yan, S. F., and Y. L. Ma. "Sensor array beampattern optimization: theory with applications." *Science, Beijing* (2009).

[18] Chen H H, Chan S C, Ho K L. “Adaptive beamforming using frequency invariant uniform concentric circular arrays,” IEEE Transactions on Circuits and Systems I: Regular Papers, 2007, 54(9): 1938-1949.

[19] D. F. Yan,“Optimal Array Signal Processing: Beamformer Design Theory and Methods”

[20] Boyd, Stephen P., and Lieven Vandenberghe. *Convex optimization*. Cambridge university press, 2004.

[21] Grant, Michael, Stephen Boyd, and Yinyu Ye. "CVX: Matlab software for disciplined convex programming." (2009).

Qianyi Ouyang was born in China, in 2002. He is currently pursuing the B.S. degree with Fudan University, Shanghai, China.

His research interests include wideband beamforming, array signal processing, and distributed beamforming.

Zhishu Qu (Member, IEEE) was born in China, in 1993. She received the B.S. and M.S. degrees in electromagnetic field and microwave technology from the University of Electronic Science and Technology of China (UESTC), Chengdu, China, in 2016 and 2019, respectively, and the Ph.D. degree in electronic engineering and computer science from the Queen Mary

University of London (QMUL), London, U.K., in 2023. She is currently a Post-Doctoral Researcher at the School of Computer Science and the Director of the Intelligent Networking and Computing Research Centre, Fudan University, China. Her research interests include satellite communications, phased arrays, and beamforming.

Yue Gao (Fellow, IEEE) received the Ph.D. degree from the Queen Mary University of London (QMUL), U.K., in 2007. He is currently a Professor at the School of Computer Science and the Director of the Intelligent Networking and Computing Research Centre, Fudan University, China. He worked as a Lecturer, a Senior Lecturer, a Reader, and the Chair Professor at QMUL and the University of Surrey, respectively. His research interests include smart antennas, sparse signal processing, and cognitive networks for mobile and satellite systems. He has published over 200 peer-reviewed journal and conference papers and had over 6400 citations. He is a member of the Board of Governors. He was also elected as an Engineering and Physical Sciences Research Council fellow in 2017. He was a co-recipient of the EU Horizon Prize Award on collaborative spectrum sharing in 2016. He is a Distinguished Speaker of the IEEE Vehicular Technology Society (VTS). He is the Vice-Chair of the IEEE ComSoc Wireless Communication Technical Committee and the past Chair of the IEEE ComSoc Technical Committee on Cognitive Networks. He has been the Symposia Chair, the Track Chair, and other roles in the organising committee of several IEEE ComSoC, VTS, and other conferences. He has been an Editor of several IEEE transactions and journals.